European Polymer Journal 71 (2015) 451–460

Contents lists available at ScienceDirect

European Polymer Journal

journal homepage: www.elsevier.com/locate/europolj

Macromolecular Nanotechnology

Remote activation by green-light irradiation of shape memory epoxies containing gold nanoparticles

A.B. Leonardi [a], J. Puig [a], J. Antonacci [b], G.F. Arenas [b], I.A. Zucchi [a], C.E. Hoppe [a], L. Reven [c], L. Zhu [d], V. Toader [c], R.J.J. Williams [a,*]

[a] Institute of Materials Science and Technology (INTEMA), University of Mar del Plata and National Research Council (CONICET), J. B. Justo 4302, 7600 Mar del Plata, Argentina
[b] Laser Laboratory, Faculty of Engineering, University of Mar del Plata. J. B. Justo 4302, 7600 Mar del Plata, Argentina
[c] Centre for Self-Assembled Chemical Structures (CSACS-CRMAA), Department of Chemistry, McGill University, 801 Sherbrooke St. W., Montreal, QC H3A 0B8, Canada
[d] Shenzhen Key Laboratory of Nano-micro Materials Research, School of Chemical Biology and Biotechnology, Peking University Shenzhen Graduate School, Shenzhen 518055, China

ARTICLE INFO

Article history:
Received 28 May 2015
Received in revised form 21 August 2015
Accepted 22 August 2015
Available online 25 August 2015

Keywords:
Epoxy nanocomposites
Gold nanoparticles
Photothermal effect
Remote activation
Shape memory epoxies

ABSTRACT

Shape memory epoxies (SMEs) that can be remotely activated by the use of green light, are described. An epoxy matrix based on on diglycidylether of bisphenol A (DGEBA cured with a mixture of *n*-dodecylamine (DA) and *m*-xylylenediamine (MXDA), exhibits excellent shape memory properties as described in a previous paper (Leonardi et al., 2011). Au NPs with an average diameter close to 5 nm could be uniformly dispersed in this matrix using poly(ethylene oxide) (PEO) chains as stabilizer. These NPs showed a significant photothermal effect even at very low concentrations (0.01 wt% as metallic gold), when irradiated with a 532 nm laser at a power close to 2 W/cm^2. Under these conditions, a bended bar (1.4-mm thickness) recovered its initial shape in a few seconds. This formulation may be used to build up devices with the necessary mechanical strength and with the possibility to produce shape recovery by remote activation using green light. A second example was analyzed employing an amphiphilic epoxy matrix to produce a uniform dispersion of Au NPs stabilized with dodecyl chains (average diameter close to 3 nm). A bar (1.4-mm thickness) of the SME with 0.04 wt% Au NPs (as metallic gold) showed a fast recovery of its initial shape by irradiation with a 532 nm laser at a power close to 2 W/cm^2. This example shows the feasibility of adapting the epoxy chemistry to disperse Au NPs stabilized with different ligands and obtained through robust synthetic methods.

1. Introduction

Among the families of shape memory polymers, shape memory epoxies (SMEs) are receiving increasing interest for practical applications due to their excellent mechanical and thermal properties, easy processability, very good shape fixing and fast recovery, and the versatility to vary the location of the glass transition temperature (T_g) [1–14]. In SMEs a temporary shape is produced at temperatures above T_g by exerting a force, it is fixed by cooling below T_g while keeping the force, and the initial shape is recovered by removing the force and heating again above T_g.

* Corresponding author.
E-mail address: williams@fi.mdp.edu.ar (R.J.J. Williams).

http://dx.doi.org/10.1016/j.eurpolymj.2015.08.024
0014-3057/

While direct heating is the usual way to activate shape recovery, some applications need remote activation. Photothermal and photochemical methods, induction heating and ultrasound activation, employed for this purpose, have been discussed in a recent review [15]. Among these methods, photothermal activation is a general approach that requires the dispersion of appropriate light absorbers in the polymer, capable of converting photons into heat. Different types of absorbers can be employed such as inks and organic dyes [16,17], gold nanoparticles or nanorods [18–23], graphene [24–26], carbon nanotubes [27], and metal complexes [28,29]. The excitation wavelength depends on the absorber type and can vary from the near IR, the visible or the UV range. One important aspect of photothermal activation is that it can produce a spatially controlled recovery toward the initial shape [16,19,22].

There are few reports of remote activation of SMEs in the literature. Puig et al. reported the synthesis of a SME containing a uniform dispersion of magnetite nanoparticles that was remotely activated in an alternating magnetic field [30]. He et al. synthesized an epoxy-based nanocomposite containing both carbon nanotubes and magnetite nanoparticles, located in different microphases [31]. As carbon nanotubes and magnetite nanoparticles responded to different radiofrequencies, both microphases could be independently activated leading to a multiple shape memory behavior. Wu et al. recently reported the synthesis of an UV/heat dual responsive SME incorporating an UV-heat transfer compound into the epoxy matrix [32]. However, no references of SMEs responsive to visible light were found. These materials can be obtained by dispersing Au nanoparticles (NPs) in the epoxy matrix. Due to the high extinction coefficient of Au NPs [33], photothermal activation would need a very small concentration of these nanoparticles [27]. In turn, this assures good transparency and improved light penetration.

An epoxy matrix based on diglycidylether of bisphenol A (DGEBA) cured with a mixture of *n*-dodecylamine (DA) and *m*-xylylenediamine (MXDA), was selected for this study. Its shape memory properties were analyzed in a previous publication [8]. This formulation exhibited interesting properties to constitute the basis of an SME. Its glass transition temperature (T_g) could be varied in a broad range by changing the DA/MXDA ratio. It varied from 14 °C (neat DA) to 120 °C (neat MXDA). The particular formulation synthesized with a molar ratio DA/MXDA = 4, with T_g = 41 °C, could be strained up to 75% in repeated shape memory cycles with tensile stresses close to 3 MPa. This formulation combined large strains with relatively large stresses, a desirable property for an SME. Shape fixity and shape recovery values were close to 98% and 96%, respectively. In order to produce remote activation of shape recovery it was necessary to disperse Au NPs in this epoxy matrix.

There are considerable challenges in achieving uniform dispersions of Au NPs in cured epoxies. One possible way is the use Au NPs with stabilizing ligands that assure solubility in the initial formulation and throughout the polymerization. In some cases, Au NPs are soluble in the monomers but segregate during reaction by a polymerization-induced phase separation process [34,35]. In order to avoid phase separation, the stabilizing ligands must be extremely soluble during the whole conversion range. Poly(ethylene oxide) (PEO) exhibits this behavior, particularly with typical epoxies based on diglycidylether of bisphenol A (DGEBA) [36–39]. Therefore, Au NPs stabilized with PEO chains were synthesized and dispersed in the epoxy monomers. The quality of the dispersion of Au NPs in the cured specimens was analyzed as well as their remote activation by irradiation with a 532 nm laser.

A second formulation was analyzed employing an amphiphilic epoxy matrix to produce a uniform dispersion of Au NPs stabilized with dodecyl chains. These NPs were synthesized with the Brust–Schiffrin classic method [40]. The amphiphilic epoxy host was described in a previous publication [41]. In this case, only the remote shape recovery by irradiation with a 532 nm laser will be reported, without any analysis of shape memory properties of the epoxy matrix. The aim of this second example was to show the feasibility of obtaining remotely activated SMEs by adapting the epoxy chemistry to disperse Au NPs stabilized with different types of ligands.

2. Experimental section

2.1. Synthesis of Au NPs coated with PEO chains (Au@PEO)

Au NPs coated with PEO chains (Au@PEO) were synthesized using a technique reported by Rucareanu et al. [42]. Briefly, a solution of tetraoctylammonium bromide (TOAB, Sigma–Aldrich) in toluene (56 mM) was contacted with an aqueous solution of $HAuCl_4 \cdot 3H_2O$ (Sigma–Aldrich, 37 mM). This mixture was stirred at room temperature until the latter was phase-transferred to the organic phase (evidenced by the decoloration of the previously yellow aqueous phase). A fresh sodium borohydride aqueous solution ($NaBH_4$, Sigma–Aldrich, 462 mM) was then added as reducing agent. After stirring overnight at room temperature, the organic layer was extracted and washed with Millipore water (three times) and then dried over anhydrous sodium sulfate. The solution was then diluted to 250 mL. The ligand (TOAB) was immediately exchanged by 4-(dimethylamino)pyridine (DMAP, Sigma–Aldrich) by adding an aqueous solution of DMAP (0.1 M) to the solution of Au@TOAB nanoparticles in toluene. Phase transfer of the particles occurred spontaneously, and the wine red aqueous solution of DMAP-stabilized Au nanoparticles (Au@DMAP), was isolated. The solution, stored at 4 °C, was stable for months. Finally, same volumes (about 125 mL) of aqueous solution (0.45 mM) of thiol-terminated poly(ethylene oxide) (PEO-SH) (M_n = 2100 g/mol) and aqueous solution of Au@DMAP were contacted overnight to promote the exchange. The volume was reduced by roto-evaporation, thereby obtaining a concentrated solution of nanoparticles. Dialysis was performed to purify the nanoparticles, using a Sephadex LH-20 membrane (MWCO 12-14000). Once the purification process was finished, Au@PEO NPs were dried combining roto-evaporation with freeze drying.

2.2. Synthesis of the shape memory epoxy (SME) containing Au@PEO NPs

The SME was obtained by reacting diglycidyl ether of bisphenol A (DGEBA, Der 332 Dow, with an epoxy equivalent mass equal to 174 g/eq), with *n*-dodecylamine (DA, Fluka, 98 wt%) and *m*-xylylenediamine (MXDA, Sigma–Aldrich), in molar ratios DGEBA:DA:MXDA equal to 6:4:1 [8]. Chemical structures of these monomers are shown in Fig. 1.

Variable amounts of Au@PEO NPs were dissolved in DGEBA at 60 °C under stirring (without using any solvent). DA was heated at 130 °C for 30 min to remove any spurious CO_2 content. Then it was mixed with the previous blend under vigorous stirring at 100 °C. Finally, the appropriate amount of MXDA was added. The mixture was placed between two Teflon-covered glass plates using a 1.4 mm-thickness rubber spacer. The polymerization was performed at 60 °C for 1 h, followed by 2 h at 80 °C, to carry the reaction to full conversion [8].

2.3. Synthesis of Au NPs coated with dodecyl chains (Au@DD)

Au NPs coated with dodecyl chains (Au@DD) were obtained by the Brust–Schiffrin classic technique [40]. Briefly, an aqueous solution containing 0.1 mmol of $HAuCl_4.3H_2O$ was mixed with a solution of TOAB (244 mg) in toluene (10 mL). The two-phase mixture was stirred until no coloration was observed in the aqueous phase. Then, 0.1 mmol of dodecanethiol was added to the organic solution followed by an excess of a freshly prepared sodium borohydride aqueous solution. The Au@DD NPs were precipitated with ethanol, added in a 7:1 volume ratio with respect to the toluene solution, followed by centrifugation (8000 rpm). The wet product was dried at 40 °C and stored at room temperature as a waxy solid.

2.4. Synthesis of a linear amphiphilic polymer (LAP)

Stoichiometric amounts of DGEBA and DA were mixed by vigorous stirring at 100 °C and kept 3 h at this temperature. A linear amphiphilic polymer (LAP) was obtained, with a repeating unit shown in Fig. 2. Its number-average molar mass, determined by size exclusion chromatography based on polystyrene standards, was M_n = 16,800 [34].

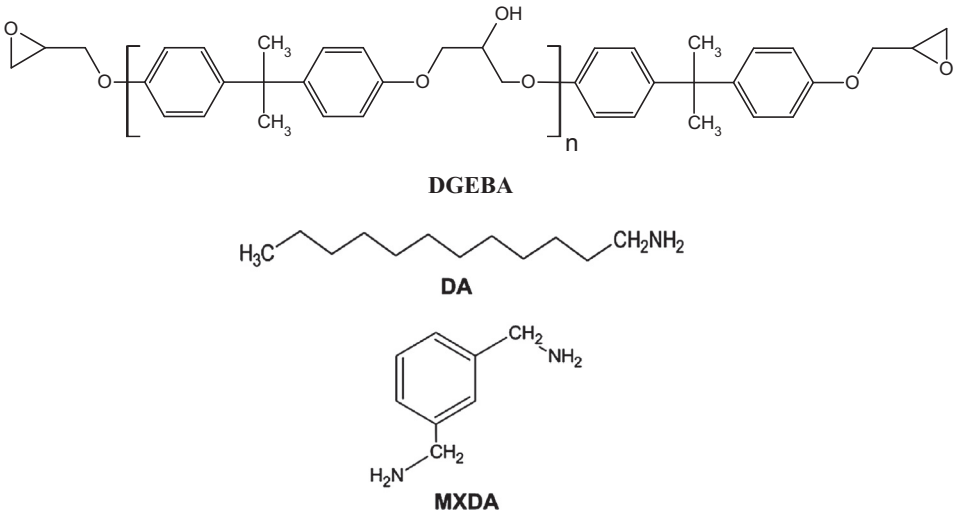

Fig. 1. Chemical structures of the monomers used for the SME containing Au@PEO NPs.

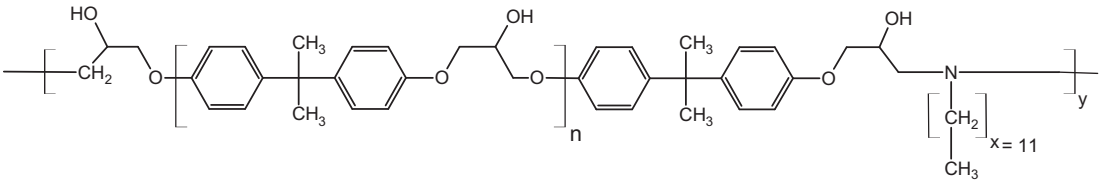

Fig. 2. Chemical structure of the linear amphiphilic polymer (LAP).

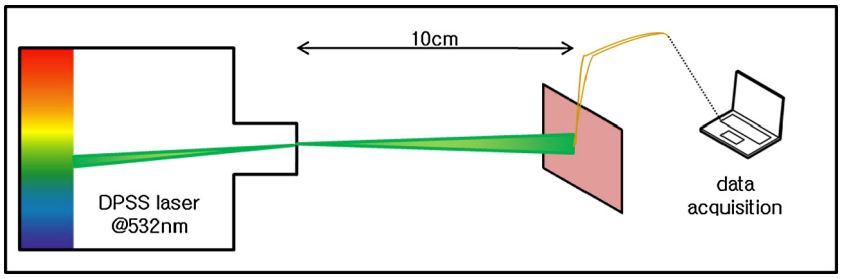

Fig. 3. Device used for the photothermal activation of SMEs.

2.5. Synthesis of the shape memory epoxy containing Au@DD NPs

DGEBA and LAP (5 wt% with respect to DGEBA) were dissolved in tetrahydrofuran (THF, in a 1:3 volume ratio) at room temperature, followed by solvent evaporation. Then, Au@DD NPs (0.04 wt% in the final formulation, expressed as metallic gold) were dispersed in a small amount of THF and blended with the mixture of DGEBA and LAP. After solvent evaporation, benzyldimethylamine (BDMA, Sigma–Aldrich, >99%) was added in a molar ratio BDMA:epoxy groups equal to 0.06. The solution was cast between two Teflon-covered glass plates using a 1.4 mm-thickness rubber spacer. Cure was performed at 100 °C for 4 h to attain complete conversion of the epoxy groups [41]. In this process, LAP was covalently bonded to the polymer network through chain transfer reactions involving the OH groups present in its repeating unit (Fig. 2). In this way, no phase separation was observed and colored transparent nanocomposites were obtained [41].

2.6. Characterization techniques

UV–visible spectra of solutions of NPs and of nanocomposites were recorded at room temperature with an Agilent 8453 diode array spectrophotometer.

Thermal gravimetric analysis (TGA) was carried out in a Shimadzu TGA-50 device, in air, at a heating rate of 10 °C/min.

Glass transition temperatures (T_g) were determined by differential scanning calorimetry (DSC, Pyris 1 Perkin-Elmer, rate = 10 or 20 °C/min). T_g was defined at the onset of the change in the specific heat.

SAXS spectra were obtained at room temperature on a small-angle X-ray scattering station (beamline SAXS 1) of the National Laboratory of Synchrotron Light (LNLS, Campinas, Brazil). The scattering intensity (in arbitrary units) was recorded as a function of the scattering vector, $q = (4\pi/\lambda)\sin(\theta)$, where λ is the radiation wavelength (1.55 Å) and 2θ the scattering angle.

Transmission electron microscope (TEM) images were obtained using a Philips CM-12 device, operated at an accelerating voltage of 100 kV. Ultrathin sections were cut with a cryo-ultramicrotome. The size distribution of NPs, their average size and the standard deviation, were determined using Image J software.

Photothermal activation of the SMEs was performed using a 1000 mW DPSS laser at 532 nm (SDL-532-1000T Shanghai Dream Lasers Technology Co. Ltd.), operated using a power control. The beam could be expanded to a spot of a diameter close to 1 cm (Fig. 3). Alternatively, a collimating lens was employed to generate a beam of 7 mm in diameter. Intensity was measured at the sample location using a sensor power meter (Silicon sensor PD200 from Ophir). The internal average temperature of the samples was measured by means of embedded T-thermocouples. Temperature was registered every 1 s with a 16 bits data acquisition system with cold junction compensation. Shape recovery was determined from recorded video observations (Samsung Galaxy S3), employing a red filter. Blank tests were performed with neat epoxy matrices without Au NPs verifying that laser irradiation did not produce any temperature increase.

3. Results and discussion

3.1. SMEs with Au@PEO NPs

The metallic gold content of Au@PEO NPs was 49 wt%, determined by TGA. An UV–visible spectrum in water is shown in Fig. 4. A clear plasmon band is observed with a maximum at 512 nm.

TEM images of SMEs containing different amounts of Au@PEO NPs (expressed as wt% of metallic gold), are shown in Fig. 5. A scale bar of 200 nm was selected to illustrate the uniform dispersion of NPs in the epoxy matrix.

The average size of NPs in these samples was determined employing Image J software (Table 1). Within the experimental error of this determination, we can assess that NPs kept their initial sizes (average close to 5 nm) without any evidence of coalescence in the more concentrated formulations.

An independent assessment of the absence of coalescence of Au NPs was obtained from SAXS spectra in the Guinier region [43]. Fig. 6 shows a set of SAXS spectra of the SMEs containing different amounts of Au@PEO NPs. Guinier plots ($\ln I$ vs q^2) in the low-q region, gave parallel straight lines with a negative slope ($-s$) for the different samples (Fig. 7).

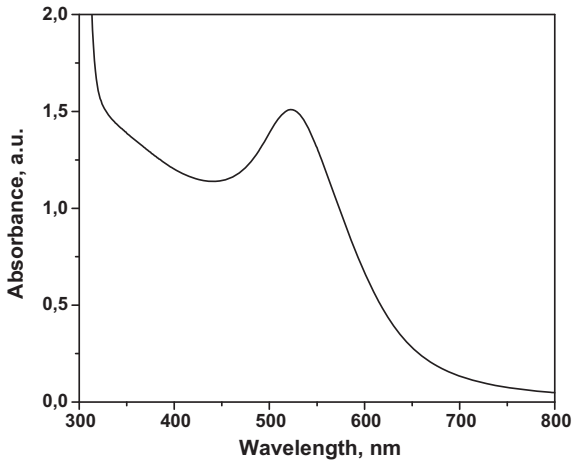

Fig. 4. UV–visible spectrum of Au@PEO NPs in aqueous solution.

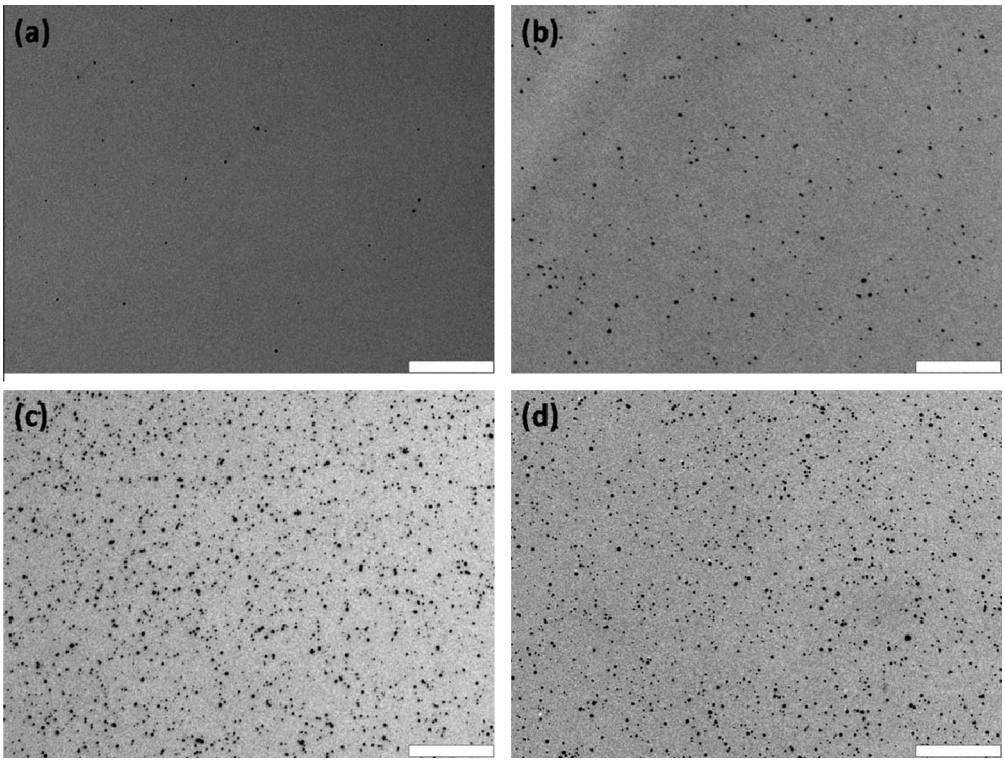

Fig. 5. TEM images of SMEs containing different amounts of Au@PEO NPs. (a) 0.05 wt%, (b) 0.1 wt%, (c) 0.5 wt%, (d) 0.75 wt%. Scale bar = 200 nm.

The radius of gyration of the nanoparticles is given by $R_g = (3s)^{1/2}$ and their radius by $R = (5/3)^{1/2}R_g = D/2$. The resulting values of diameters are shown in Table 1. For a polydisperse set of spherical objects the Guinier-average diameter is close to the diameter of the largest objects of the population. This agrees with the size of the largest nanoparticles observed in TEM images (from about 7–10 nm).

The shape memory properties of the epoxy matrix were discussed in a previous publication [8]. The matrix with a $T_g = 41$ °C, could be strained up to 75% in repeated shape memory cycles with tensile stresses close to 3 MPa. Shape fixity and shape recovery values were close to 98% and 96%, respectively. We assumed that the small amount of Au@PEO NPs did not produce any significant change in thermal and mechanical properties of the matrix. In particular, we verified that the glass transition temperatures of the different nanocomposites was the same as the one of the matrix.

Table 1
Average diameters of Au@PEO NPs (gold cores) obtained from TEM images and from Guinier plots.

wt% NPs[a]	D_{TEM} (nm)[b]	$D_{Guinier}$ (nm)[c]
0.01	–	7.6
0.05	5.3 ± 1.5	–
0.1	4.8 ± 1.4	7.6
0.5	4.5 ± 1.6	7.6
0.75	4.4 ± 1.6	7.6

[a] Expressed as metallic gold.
[b] Average diameter of the gold cores determined from TEM images with the corresponding standard deviation.
[c] Diameter of the gold cores determined from Guinier plots.

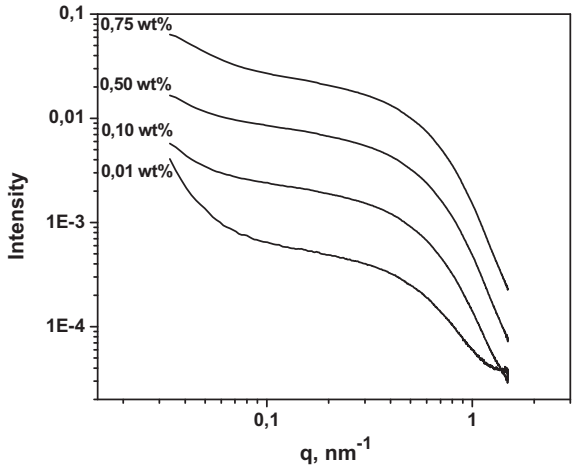

Fig. 6. SAXS spectra of SMEs containing different amounts of Au@PEO NPs.

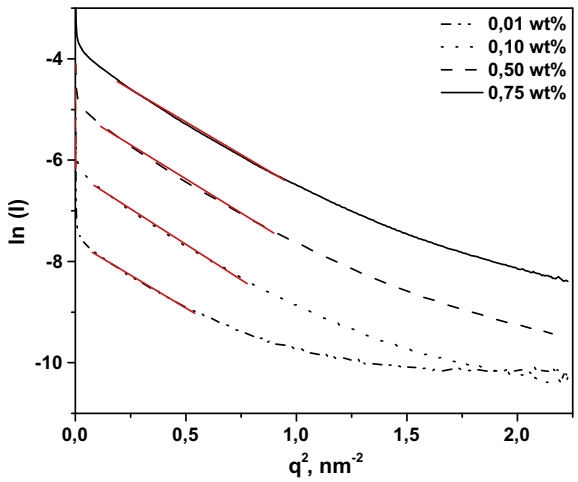

Fig. 7. Guinier plots indicating the linear region used to determine the diameter of NPs.

In order to produce shape recovery it was necessary to verify that green-light irradiation increased temperature beyond the glass transition. A T-thermocouple was placed close to the center of the mold (1.4 mm thickness) before the cure so that it became embedded in the final material. The temperature increase produced by green-light irradiation (power density close to 2 W/cm^2) of samples containing 0.01, 0.05 and 0.1 wt% Au@PEO NPs, is shown in Fig. 8. Very large temperature

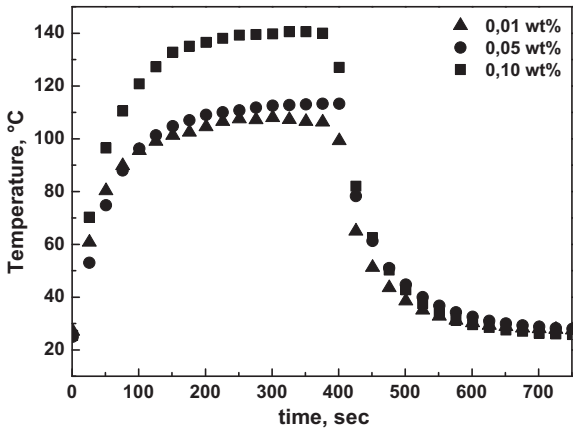

Fig. 8. Temperature increase recorded for SMEs containing different amounts of Au@PEO NPs. Temperature was recorded with a thermocouple inserted in the material before polymerization.

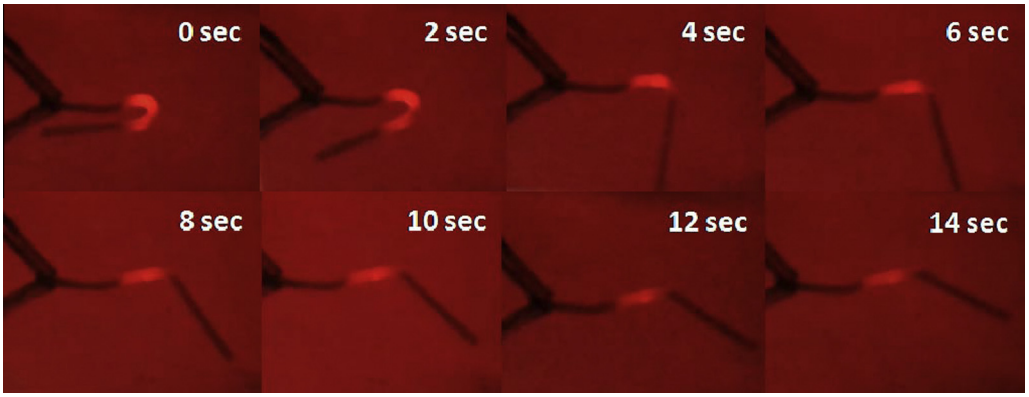

Fig. 9. Shape recovery of a bar of a SME containing 0.01 wt% Au@PEO NPs, previously folded 180°, when irradiated with green light at the curvature (photos taken with a red filter). (For interpretation of the references to color in this figure legend, the reader is referred to the web version of this article.)

increases were observed for every sample, attaining values as high as 140 °C for the SME with 0.1 wt% Au@PEO NPs. Besides, no temperature increase was observed when irradiating the neat SME, meaning that the generated heat must be exclusively ascribed to the photothermal effect. Temperature attained asymptotic values after about 300 s irradiation, meaning that a steady state was attained compensating heat generation by heat dissipation. However, the glass transition temperature (41 °C) was surpassed after a few seconds even for the sample containing the smallest amount of NPs. A sharp temperature decrease was observed when stopping the irradiation.

It is interesting to compare these results with those recently reported by Zhang and Zhao [21] for a shape memory polymer based on a crosslinked PEO containing 0.003 wt% Au@PEO NPs. These NPs had a metallic core of 10 nm and a similar length of stabilizing ligands as those synthesized in the present study. They were able to increase temperature of a 0.4-mm film to 75 °C, by irradiating with green light at a power density of 5 W/cm^2. In a following paper [22], they synthesized 1-mm films of the same material containing 0.5 wt% Au@PEO NPs and showed the possibility of generating temperature gradients in the specimen by irradiating with a power density close to 2 W/cm^2.

In order to prove that shape recovery can be produced remotely by green-light irradiation, the smallest concentration of NPs was selected to assure good transparency and improved light penetration. A bar (45 × 5 × 1.4 mm) of the SME containing 0.01 wt% Au@PEO NPs was heated to 50 °C and bended. The bar was then cooled to room temperature while keeping the deformation. It was placed in the device shown in Fig. 3 and the curved portion of the sample was irradiated with the green laser. Fig. 9 shows that shape recovery occurred after a few seconds (the experience was arrested after 14 s irradiation; to continue shape recovery it would have been necessary to shift slightly the irradiation area).

3.2. SMEs with Au@DD NPs

Fig. 10 shows UV–visible spectra of the original Brust NPs in a THF solution (dashed line) and of the SME containing 0.05 wt% Au@DD NPs (continuous line). The average size of Au@DD NPs synthesized by the Brust technique was close to

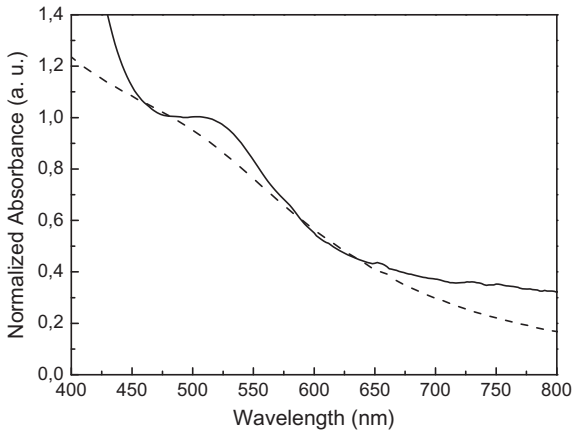

Fig. 10. UV–visible spectrum of Au@DD NPs in a THF solution (dashed line) and of the SME containing 0.05 wt% Au@DD NPs (continuous line).

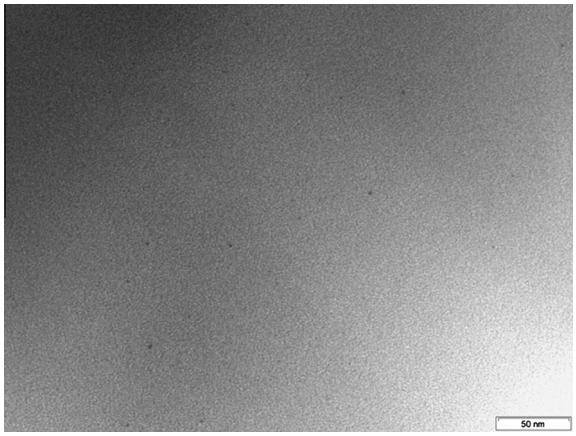

Fig. 11. TEM image of the SME containing 0.04 wt% Au@DD NPs. The scale bar represents 50 nm.

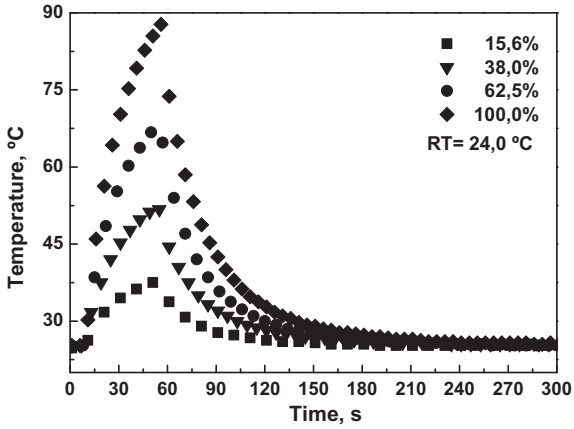

Fig. 12. Temperature increase in the SME with 0.04 wt% Au@DD NPs recorded with an embedded thermocouple. The irradiation started at 10 s and was stopped at 52 s. Curves correspond to different irradiation powers (100% corresponds to about 700 mW).

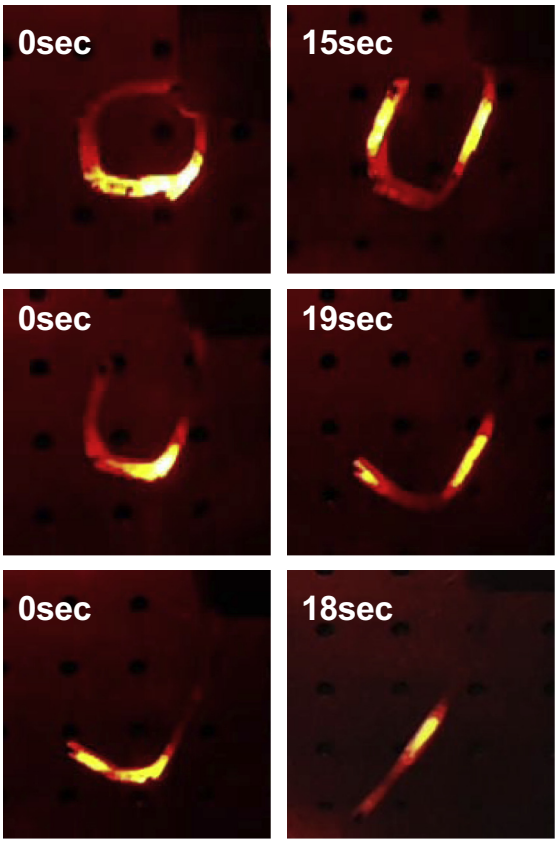

Fig. 13. Shape recovery of the SME with 0.04 wt% Au@DD NPs by irradiating with green light at the previously bended sections (photographs taken with a red filter). The first irradiation step was carried out for 15 s at the first bended section; the second step was performed for 19 s at the second bended section, and the last step for another 18 s at the third bended section. This enabled a complete recovery of the initial shape. (For interpretation of the references to color in this figure legend, the reader is referred to the web version of this article.)

2 nm and the contents of metallic gold determined by TGA, was 78% [34]. According to this small size, the plasmon band of the NPs in the THF solution was barely discernible. However, its intensity was higher in the SME, a fact assigned to a partial coalescence of NPs during polymerization at 100 °C [34]. The average diameter of Au@DD NPs, obtained by processing TEM images, was 2.8 ± 0.7 nm. As an example, Fig. 11 shows one of these TEM images with a few NPs present as small black domains.

The glass transition temperature of the SME was 43 °C. Therefore, it was necessary to heat above this temperature by green light irradiation to produce shape recovery. Fig. 12 shows the temperature increase in the SME recorded with an embedded thermocouple. Curves correspond to different irradiation powers (100% corresponds to 700 mW equivalent to about 2 W/cm^2 at the sample surface). When employing 38% or more of the maximum power, temperature increased over the glass transition in less than 30 s. At the maximum power, only a few seconds were necessary to surpass the glass transition temperature. This is a significant result considering the low intensity of the plasmon band. A sharp temperature decrease was observed when stopping the irradiation.

In order to prove that green-light irradiation could produce shape recovery, a bar (50 × 5 × 1.4 mm) of the SME was heated above the glass transition temperature and bended in three different sections to obtain a rounded form (temporary shape). Fig. 13 shows the shape recovery of the bar when it was irradiated with the green laser at each one of the bended sections. The first irradiation step was carried out for 15 s at the first bended section; the second step was performed for 19 s at the second bended section, and the last step for another 18 s at the third bended section. This enabled a complete recovery of the initial shape.

4. Conclusions

To the best of our knowledge, this is the first study describing shape memory epoxies that can be remotely activated by the use of green light. An epoxy matrix based on DGEBA cured with a mixture of amines (MXDA and DA) exhibits excellent shape memory properties as described in a previous paper [8]. Au NPs with an average diameter close to 5 nm could be

uniformly dispersed in this matrix using PEO chains as stabilizer. These NPs showed a significant photothermal effect even at very low concentrations (0.01 wt% as metallic gold), when irradiated at a power close to 2 W/cm^2. Under these conditions, a bended bar (1.4-mm thickness) recovered its initial shape in a few seconds. This particular material with excellent shape memory properties may be used to build up devices with the necessary mechanical strength and with the possibility to produce shape recovery by remote activation using green light.

A second example was presented to show the feasibility of adapting the epoxy chemistry to disperse Au NPs with different kinds of stabilizing ligands. This enables to use robust synthetic methods of Au NPs combined with adaptable epoxy chemistries to produce their uniform dispersion.

Finally, a significant result of both cases is the fact that low concentrations of small Au NPs (average size close to 5 nm in the first case and to 3 nm in the second one) have enough photothermal activity to produce remote shape recovery by green-light irradiation.

Acknowledgements

Authors thank the financial support of the following institutions: University of Mar del Plata (Argentina), National Research Council (CONICET, Argentina) and National Agency for the Promotion of Science and Technology (ANPCyT, Argentina). J. Puig acknowledges the postdoctoral scholarship awarded by Fundación Bunge y Born (Argentina). Fonds de Recherche du Quebec Nature et Technologies (FQRNT) supported the contribution of L. Zhu, V. Toader and L. Reven. The grant SAXS1-17067 from the Brazilian Synchrotron Light Laboratory (LNLS, Campinas, Brazil) is gratefully acknowledged.

References

[1] P.T. Mather, X. Luo, I.A. Rousseau, Annu. Rev. Mater. Res. 39 (2009) 445–471.
[2] M. Behl, J. Zotzmann, A. Lendlein, Adv. Polym. Sci. 226 (2010) 1–40.
[3] T.H. Tong, B.J. Vining, R.D. Hreha, T.J. Barnell, Shape memory epoxy copolymer, US Patent 2008/0269420.
[4] T. Xie, I.A. Rousseau, Polymer 50 (2009) 1852–1856.
[5] I.A. Rousseau, T. Xie, J. Mater. Chem. 20 (2010) 3431–3441.
[6] D.M. Feldkamp, I.A. Rousseau, Macromol. Mater. Eng. 295 (2010) 726–734.
[7] Y. Liu, C. Han, H. Tan, X. Du, Mater. Sci. Eng., A 527 (2010) 2510–2514.
[8] A.B. Leonardi, L.A. Fasce, I.A. Zucchi, C.E. Hoppe, E.R. Soulé, C.J. Pérez, R.J.J. Williams, Eur. Polym. J. 47 (2011) 362–369.
[9] S. Pandini, F. Bignotti, F. Baldi, S. Passera, J. Intell. Mater. Syst. Struct. 24 (2013) 1583–1597.
[10] A.H. Torbati, H.B. Nejad, M. Ponce, J.P. Sutton, P.T. Mather, Soft Matter 10 (2014) 3112–3121.
[11] Y. Dong, Q.Q. Ni, L. Li, Y. Fu, Mater. Lett. 132 (2014) 206–209.
[12] M. Fan, X. Li, J. Zhang, J. Cheng, J. Thermal Anal. Calorim. 119 (2015) 537–546.
[13] Y. Dong, Q.Q. Ni, Y. Fu, Compos. Part A: Appl. Sci. Manuf. 72 (2015) 1–10.
[14] W. Wang, D. Liu, Y. Liu, J. Leng, D. Bhattacharyya, Compos. Sci. Technol. 106 (2015) 20–24.
[15] G.J. Berg, M.K. McBride, C. Wang, C.N. Bowman, Polymer 55 (2014) 5849–5872.
[16] Y. Liu, J.K. Boyles, J. Genzer, M.D. Dickey, Soft Matter 8 (2012) 1764–1769.
[17] Y. Liu, M. Miskiewicz, M.J. Escuti, J. Genzer, M.D. Dickey, J. Appl. Phys. 115 (20) (2014).
[18] K.C. Hribar, R.B. Metter, J.L. Ifkovits, T. Troxler, J.A. Burdick, Small 5 (2009) 1830–1834.
[19] H. Zhang, H. Xia, Y. Zhao, J. Mater. Chem. 22 (2012) 845–849.
[20] H. Zhang, J. Zhang, X. Tong, D. Ma, Y. Zhao, Macromol. Rapid Commun. 34 (2013) 1575–1579.
[21] H. Zhang, Y. Zhao, ACS Appl. Mater. Interfaces 5 (2013) 13069–13075.
[22] H. Zhang, H. Xia, Y. Zhao, ACS Macro Lett. 3 (2014) 940–943.
[23] D.B. Abbott, S. Maity, M.T. Burkey, R.E. Gorga, J.R. Bochinski, L.I. Clarke, Macromol. Chem. Phys. 215 (2014) 2345–2356.
[24] Y. Feng, M. Qin, H. Guo, K. Yoshino, W. Feng, Appl. Mater. Interfaces 5 (2013) 10882–10888.
[25] J. Park, B. Kim, Smart Mater. Struct. 23 (2014) 025038.
[26] M. Kashif, Y.W. Chang, Eur. Polym. J. 66 (2015) 273–281.
[27] R.R. Kohlmeyer, M. Lor, J. Chen, Nano Lett. 12 (2012) 2757–2762.
[28] J.R. Kumpfer, S.J. Rowan, J. Am. Chem. Soc. 133 (2011) 12866–12874.
[29] H. Xia, Z. Wang, W. Fang, R. Tong, X. Lu, RSC Adv. 4 (2014) 25486–25493.
[30] J. Puig, C.E. Hoppe, L.A. Fasce, C.J. Pérez, Y. Piñeiro-Redondo, M. Bañobre-López, M.A. López-Quintela, J. Rivas, R.J.J. Williams, J. Phys. Chem. C 116 (2012) 13421–13428.
[31] Z. He, N. Satarkar, T. Xie, Y.T. Cheng, J.Z. Hilt, Adv. Mater. 23 (2011) 3192–3196.
[32] Y. Wu, J. Hu, C. Zhang, J. Han, Y. Wang, B. Kumar, J. Mater. Chem. A 3 (2015) 97–100.
[33] S. Eustis, M.A. El-Sayed, Chem. Soc. Rev. 35 (2006) 209–217.
[34] I.A. Zucchi, C.E. Hoppe, M.J. Galante, R.J.J. Williams, M.A. López-Quintela, L. Matějka, M. Slouf, J. Pleštil, Macromolecules 41 (2008) 4895–4903.
[35] R.J.J. Williams, C.E. Hoppe, I.A. Zucchi, H.E. Romeo, I.E. dell'Erba, M.L. Gómez, J. Puig, A.B. Leonardi, J. Colloid Interface Sci. 431 (2014) 223–232.
[36] S. Zheng, N. Zhang, X. Luo, D. Ma, Polymer 36 (1995) 3609–3613.
[37] Q. Guo, C. Harrats, G. Groeninckx, M.H.J. Koch, Polymer 42 (2001) 4127–4140.
[38] F. Meng, S. Zheng, H. Li, Q. Liang, T. Liu, Macromolecules 39 (2006) 5072–5080.
[39] A.B. Leonardi, I.A. Zucchi, R.J.J. Williams, Eur. Polym. J. 65 (2015) 202–208.
[40] M. Brust, M. Walker, D. Bethell, D.J. Schiffrin, R. Whyman, Chem. Commun. 7 (1994) 801–802.
[41] J. Puig, I.A. Zucchi, C.E. Hoppe, M.A. López-Quintela, R.J.J. Williams, Colloid Polym. Sci. 291 (2013) 1677–1682.
[42] S. Rucareanu, M. Maccarini, J.L. Shepherd, R.B. Lennox, J. Mater. Chem. 18 (2008) 5830–5834.
[43] A. Guinier, G. Fournet, Small-angle scattering of X-rays, Wiley, New York, 1955.